J Paleolimnol (2012) 48:259–273
DOI 10.1007/s10933-012-9604-7

ORIGINAL PAPER

Evaluating Holocene climate change in northern Norway using sediment records from two contrasting lake systems

Nicholas L. Balascio · Raymond S. Bradley

Received: 31 August 2011 / Accepted: 15 March 2012 / Published online: 22 April 2012

Abstract We analyzed Holocene sedimentary records from two lakes in the Lofoten Islands, northern Norway to evaluate environmental changes during the Holocene related to northern North Atlantic climate dynamics. The lakes are located in different geomorphological settings, and thus provide a contrast in their response to regional climate change. Environmental changes at both lakes were interpreted based on magnetic susceptibility, organic-matter flux, C/N, $\delta^{13}C_{org}$, Ti concentrations, and mass accumulation rates. Chronologies were established using 16 AMS radiocarbon dates, and average deposition rates in both environments are higher than 0.2 mm/year throughout the Holocene. At Vikjordvatnet, sedimentary geochemical properties define three distinct phases of sedimentation related to changes in aquatic productivity and gradual landscape development. Following deglaciation, during the early Holocene (11.6–7.2 ka), aquatic productivity increased and the landscape stabilized as regional temperatures increased in response to higher summer insolation and increasing inflow of warm Atlantic water into the Norwegian Sea. Centennial-scale intervals of decreased organic-matter flux, from 10.9 to 10.2 ka and 9.2 to 8.0 ka, record episodes of instability during the early Holocene. These may represent regional cooling events related to freshwater forcing and a slowdown of the northward transport of warm water into the North Atlantic. During the mid-Holocene (7.2–4.8 ka) organic-matter properties show less variability and the timing of this phase corresponds with the regional Holocene thermal maximum. The late Holocene sediments (4.8 ka–present) record a transition to colder climate conditions. The record from Fiskebølvatnet captures periodic changes in clastic input related to runoff and exhibits high-frequency variations over the last 9.5 ka. The most significant change in sedimentation was during the late Holocene (4.3 ka–present) when the frequency and magnitude of runoff events show an abrupt transition to wetter conditions. The timing of this shift corresponds to other regional reconstructions that indicate wetter and colder conditions during the late Holocene.

Keywords Lake sediment · Paleoclimate · Holocene · Lofoten Islands · Norway

This is one of 18 papers published in a special issue edited by Darrell Kaufman, and dedicated to reconstructing Holocene climate and environmental change from Arctic lake sediments.

N. L. Balascio (✉) · R. S. Bradley
Climate System Research Center, Department of Geosciences, University of Massachusetts, Amherst, MA 01003, USA
e-mail: balascio@geo.umass.edu

Introduction

Holocene paleoenvironmental reconstructions provide information on the natural variability of the climate system and provide longer-term perspectives on present climate trends (Bradley 2008). In the Arctic,

the principal features of Holocene climate are two multi-millennial-scale intervals: the early Holocene thermal maximum, and the late Holocene Neoglacial period, which was marked by the expansion of mountain glaciers and ice caps (Miller et al. 2010). Regional climate reconstructions show that the onset and termination of these intervals were not spatially uniform (Kaufman et al. 2004; Miller et al. 2010). The detailed analysis of paleoclimate archives across the Arctic helps characterize the regional response during these and other Holocene climate intervals to better define the magnitude and timing of past climate changes.

Lacustrine systems are particularly useful in Holocene paleoclimate studies because of their broad geographic distribution, sensitivity to environmental changes, and continuous sedimentary sequences, which can often be well resolved. In addition, there are many physical and biological properties of lake basins and lake sediments that can be examined to interpret paleoenvironmental conditions within the water column and the surrounding landscape (Last and Smol 2001). However, the geomorphic and hydrologic setting of each lake influences the paleoenvironmental signal recorded in their sediments and needs to be assessed to determine how proxy records respond to local and regional conditions (Rubensdotter and Rosqvist 2003, 2009; Bakke et al. 2010; Corbett and Munroe 2010).

This study investigates characteristics of Holocene climate variability along the coast of northern Norway by studying two lacustrine environments in the Lofoten Islands (Fig. 1). The Lofoten Islands extend from the mainland out into the Norwegian Sea, and experience climate conditions that are influenced by major oceanic and atmospheric components of the North Atlantic climate system. Lake sediment records from this area can therefore be used to help define the response of these systems to Holocene climate changes.

We present the sedimentary records from two lakes, Vikjordvatnet and Fiskebølvatnet (Fig. 1). They are located 32 km from each other, but are within catchments that have different geomorphic and hydrologic characteristics and therefore respond differently to past climate changes. Physical and bulk organic geochemical properties were measured with a high sampling resolution to interpret the nature and timing of past changes. We interpret environmental conditions using

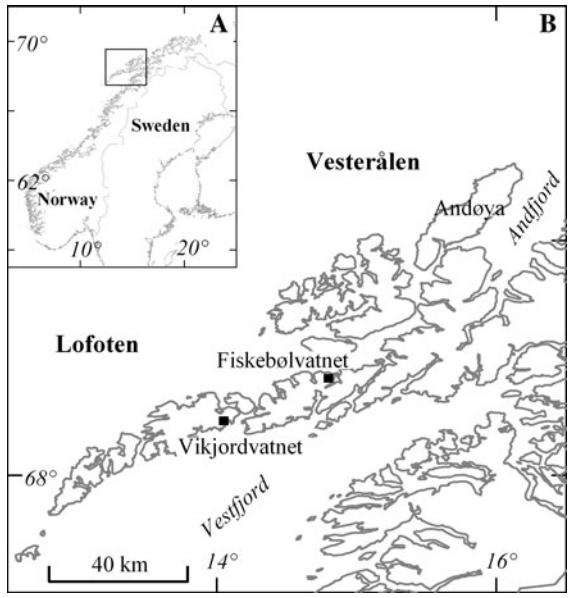

Fig. 1 Location of the Lofoten-Vesterålen archipelago off the coast of northern Norway (*a*), the location of lakes Vikjordvatnet and Fiskebølvatnet (*black squares*), and other sites mentioned in the text (*b*)

magnetic susceptibility, organic-matter flux, C/N, $\delta^{13}C_{org}$, Ti concentrations, and mass accumulation rates (MAR). These parameters provide information on the characteristics and rates of terrestrial input and autochthonous lake productivity. Examining these characteristics in two different environments allows us to more comprehensively assess past environmental conditions in this region during the Holocene.

Setting

The Lofoten-Vesterålen archipelago (67–70°N) is a chain of mountainous islands dissected by cirques, glacial valleys, and fjords that extends from northeast to southwest into the Norwegian Sea (Fig. 1). Vesterålen is the northerly chain of islands that includes Andøya, which is separated from the mainland by Andfjord. The Lofoten Islands are the southerly islands separated from the mainland by Vestfjord. Lofoten consists of seven islands and Austvågoya and Vestvågøya are the largest. The steep mountain peaks of Lofoten reach up to 1,100 m and are composed of various Precambrian intermediate to felsic plutonic

rocks and gneisses (Tveten 1978). Quaternary surficial material consists of isolated deposits of glacial till, raised marine sediments, and peat bogs.

Climate along the coast of Norway is strongly affected by northward transport of heat through oceanic and atmospheric dynamics. The Lofoten Islands experience mild conditions with mean annual temperatures of 4.7 °C and mean annual precipitation of 1,500 mm, as measured at Svolvær on the island Austvågoya from 1961 to 1990 (Norwegian Meteorological Institute, met.no). The Norwegian Current, an extension of the North Atlantic Current, carries warm water to the high latitudes of northern Norway (Hopkins 1991). The North Atlantic Oscillation also impacts the region primarily during positive phases when stronger-than-average westerly winds cause greater storminess in the Norwegian Sea increasing winter precipitation and sea-surface temperatures (Uvo 2003; Hurrell and Dickson 2004), a phenomena well expressed in records of glacier mass balance (Nesje et al. 2000).

A network of marine and terrestrial paleoclimate reconstructions is available for this region. Millennial-scale Holocene climate trends are expressed in sea-surface temperature (SST) reconstructions from the Norwegian margin and in atmospheric temperature reconstructions based on biological proxies from northern Fennoscandia. SST changes have been studied from a transect of marines cores along the continental margin based on planktonic foraminifera (Hald et al. 2007) and using multiple temperature proxies at coring site MD952011, which is located directly beneath the Norwegian Atlantic Current (Birks and Koç 2002; Calvo et al. 2002; Risebrobakken et al. 2003; Andersen et al. 2004; Berner et al. 2011). Holocene atmospheric summer temperature reconstructions for this region have also been generated from lacustrine records using pollen, chironomids, and diatoms (Korhola et al. 2000, 2002; Rosén et al. 2001; Seppä and Birks 2001, 2002; Bigler et al. 2002, 2003, 2006; Seppä et al. 2002, 2009; Bjune et al. 2004; Larocque and Bigler 2004; Heinrichs et al. 2006; Bjune and Birks 2008).

Study areas

Vikjordvatnet (68°13.64′N, 14°3.79′E; 23 m a.s.l.) is located on the southeastern coast of Vestvågøya (Fig. 1). It is a small, circular lake that is ~300 m in diameter and has a maximum water depth of 21 m. Water column chemistry profiles and temperature measurements acquired throughout 2009–2010 indicate that the lake is dimictic, similar to most lakes studied in the region. The valley above Vikjordvatnet contains a series of three lakes below an east-facing cirque with peak elevations of 540 and 589 m a.s.l. (Fig. 2). The upper two lakes are surrounded by steep valley walls and talus slopes. Lower in the catchment, the valley widens, has gentle slopes, and more

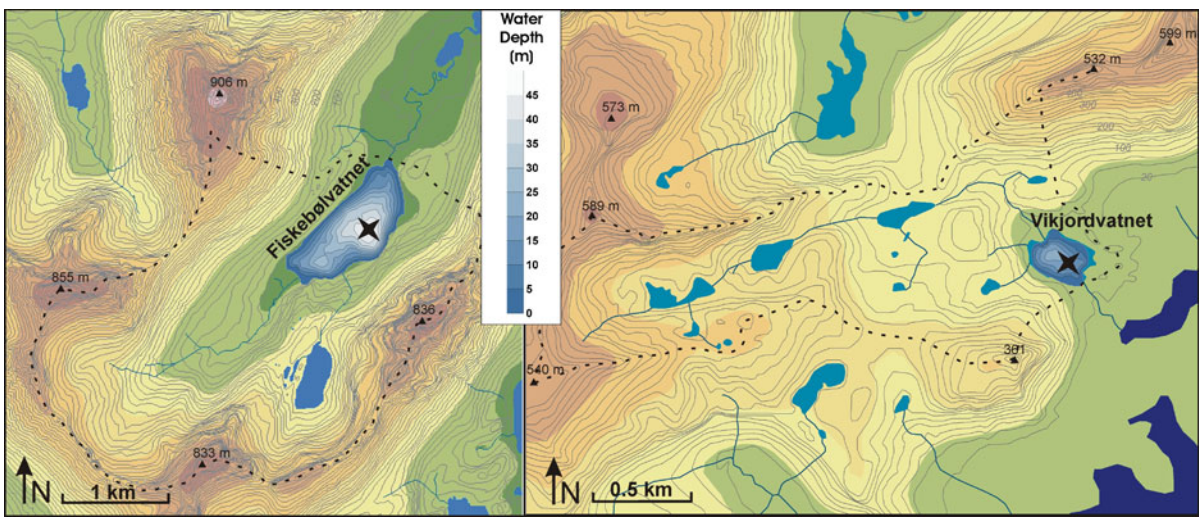

Fig. 2 Bathymetry and catchment setting of Fiskebølvatnet (*left panel*) and Vikjordvatnet (*right panel*). *Dotted lines* indicate drainage divides

complete soil and vegetation cover. Vikjordvatnet is located within a bedrock depression and drains southeast into the ocean. The elevation of the lake indicates that it is below the local marine limit, mapped at 26 m a.s.l. (Møller 1985), which was likely reached immediately following deglaciation. This elevation is similar to the marine limit farther north, near Andøya, where it is dated to between 18.5 and 15.5 ^{14}C ka BP (Fig. 1) (Vorren et al. 1988).

Fiskebølvatnet (68°24.78′N, 14°48.09′E; 23 m a.s.l.) is located on the northeastern coast of Austvågøya (Fig. 1). The lake is roughly 1 km long and 400 m wide. A water-column chemistry profile measured in 2008 is similar to other lakes studied in the region, indicating that Fiskebølvatnet is dimictic. It is within a steep-sided, northeast trending valley surrounded by mountain peaks with summit elevations from 833 to 906 m a.s.l. (Fig. 2). Soil and vegetation cover is sparse on the steepest slopes and more extensive cover is restricted to the valley floor. There are two cirques above the lake. Streams draining these areas flow into the southwestern end of Fiskebølvatnet. The eastern cirque contains a small lake that drains northward over a waterfall into Fiskebølvatnet. Fiskebølvatnet is impounded by a moraine and drains to the northeast through a broad, flat marsh before entering the ocean. There is one main basin in the middle of the lake with a maximum water depth of 44 m and one smaller basin, 24 m deep, at the southwestern end (Fig. 2). Fiskebølvatnet is below the local marine limit, mapped at 37–38 m based on raised shoreline features (Møller 1985), and was isolated from the ocean at 9.5 cal ka BP (Balascio 2011).

Methods

Sediment cores from Vikjordvatnet and Fiskebølvatnet were recovered during the summer of 2008. The sediment from Vikjordvatnet was collected as a series of overlapping drives using a Livingstone square-rod piston corer. A composite 3.01-m sequence was compiled by matching the physical stratigraphy and magnetic susceptibility profiles (Balascio 2011). The sediment from Fiskebølvatnet was collected as a single 5.73-m-long drive using a modified Nesje percussion coring device. The core was cut into ~1.4 m sections in the field. The marine-lacustrine transition in the Fiskebølvatnet core is at 3.4 m depth (Balascio 2011), and we focus on the lacustrine phase of the record for this study.

The chronologies for these cores are based on 16 AMS radiocarbon measurements on plant macrofossils (Table 1). Samples were picked from the core surface or wet sieved with deionized water. All radiocarbon ages were calibrated to calendar years using CALIB v. 6.0 (Stuiver and Reimer 1993) with the IntCal09 calibration dataset (Reimer et al. 2009). All ages are presented in calendar years prior to AD 1950 (BP) unless otherwise indicated. Age-depth models were created in R (R Development Core Team 2011) using the Clam routine (Blaauw 2010). Smooth spline functions, weighted by the probability distributions of the calibrated age ranges, were fitted to each set of ages (Blaauw 2010).

The magnetic susceptibility of the cores was measured every 0.5 cm on the cores from Vikjordvatnet and every 1 cm on the cores from Fiskebølvatnet using a Bartington MS2E sensor. Both cores were then sampled volumetrically at 1 cm intervals to measure the dry bulk density and the organic-matter content by loss-on-ignition (LOI). Dry bulk density was calculated as the mass of 1 cm^3 samples after drying for 24 h at 100 °C. Organic-matter content was calculated as the difference between the mass of the dried 1 cm^3 samples and their mass after heating for 1 h at 550 °C (Dean 1974). Dry bulk density and the calculated sedimentation rate (cm/year) were used to determine mass accumulation rates (MAR; g/cm^2/year) and organic-matter flux (OM × MAR).

Samples spanning 1-cm-depth intervals were taken every 5 cm from both cores to measure bulk organic geochemical properties. Samples were dried overnight in a low temperature oven, acidified with concentrated sulfurous acid, and analyzed for total organic carbon (TOC), total nitrogen (TN), and δ^{13}C on a Costech ECS 410 elemental analyzer interfaced with a Thermo Delta V Advantage IRMS. Isotopic values are reported in per mil (‰) notation relative to VPDB for δ^{13}C. Uncertainties in TOC and TN measurements are ±0.2 % and ±0.3 ‰ for δ^{13}C based on triplicate analysis. C/N values were calculated as the ratio of TOC to TN.

The Ti composition of both sediment cores was determined by scanning X-ray fluorescence (XRF) using an Itrax^{TM} core scanner at the University of Quebec's Institut national de la recherche scientifique, Centre Eau, Terre et Environment. The split core

Table 1 Radiocarbon ages on macrofossils from cores taken from Vikjordvatnet and Fiskebølvatnet

Laboratory ID[a]	Core depth (cm)[b]	$\delta^{13}C$ (‰)	^{14}C Age (^{14}C year BP)	Calibrated age range (cal year BP)		Median age (cal year BP)
				(1 σ)	(2 σ)	
Vikjordvatnet						
OS-80456	27	−26.02	1,400 ± 25	1,292–1,326	1,286–1,344	1,310
UCI-58697	59	–	2,435 ± 20	2,363–2,654	2,356–2,694	2,455
OS-80587	84	−22.92	3,210 ± 30	3,394–3,450	3,369–3,477	3,425
OS-80588	123	−26.68	4,250 ± 30	4,826–4,852	4,661–4,864	4,840
UCI-58698	153	–	5,065 ± 20	5,751–5,891	5,747–5,899	5,820
OS-80589	189	−26.07	6,260 ± 35	7,166–7,247	7,027–7,267	7,205
UCI-58704	208	–	7,165 ± 25	7,963–8,000	7,947–8,017	7,980
OS-80590	220	−25.79	7,890 ± 40	8,603–8,755	8,591–8,975	8,700
UCI-58699	232	–	8,430 ± 30	9,441–9,487	9,421–9,524	9,470
Fiskebølvatnet						
OS-80453	36	−30.44	1,100 ± 30	966–1,053	937–1,062	1,010
UCI-58700	109	–	2,255 ± 20	2,184–2,335	2,159–2,341	2,230
OS-80454	158	−28.62	3,270 ± 35	3,450–3,556	3,403–3,576	3,500
UCI-58701	216	–	3,960 ± 20	4,413–4,498	4,303–4,517	4,430
OS-80455	285	−27.95	6,070 ± 45	6,809–6,996	6,789–7,155	6,930
UCI-58702	325	–	8,000 ± 30	8,780–8,995	8,729–9,006	8,880
UCI-58703	338	–	8,440 ± 30	9,445–9,493	9,432–9,523	9,475

[a] *UCI* University of California Irvine Keck-CCAMS Facility; *OS* National Ocean Sciences Accelerator Mass Spectrometry Facility

[b] Sample depths are midpoints of samples 0.5–1.0 cm thick

surfaces were scanned at 0.5 cm intervals. We applied an exposure time of 50 s, voltage of 35 kV, and current of 35 nA to the Vikjordvatnet core. The Fiskebølvatnet core was analyzed with an exposure time of 50 s, voltage of 25 kV, and current of 25 nA. Across each 0.5 cm interval, dispersive energy spectrums were acquired and the peak area integrals were calculated for each element.

Results[1]

Vikjordvatnet

The 301-cm-long core from Vikjordvatnet consists of three main lithostratigraphic units (Fig. 3a). From 301 to 268 cm, the sediment is dense gray clay with faint laminations and a few thin sandy horizons. This unit abruptly transitions into a light grayish brown sequence, 268–190 cm, that grades into a darker brown color and increases in organic content from 268 to 190 cm. Within this interval there is a thin clay layer at 218 cm. Above 190, the sediment is massive, dark brown, and organic rich.

Nine radiocarbon ages define the age-depth model for the core from Vikjordvatnet (Fig. 3a). The 2-σ uncertainty ranges for the smooth spline function average ±0.07 ka for the last 9.5 ka. Before 9.5 ka, the uncertainty increases to a maximum range of ±0.7 ka years. The basal age, c. 13.7 ± 0.7 ka, and the age of the transition from clay to more organic-rich sediment at 268 cm, c. 11.6 ± 0.4 ka, are extrapolated from the lowest date, 9.5 ka (232 cm), and the associated uncertainty is greater in this part of the chronology. Cryptotephra have been found in extremely low concentrations from 261 to 263 cm (Balascio 2011). The geochemistry of glass shards isolated within this interval is similar to tephra from the Icelandic eruption of the Askja caldera c. 11 ka

[1] All of the data from lakes Vikjordvatnet and Fiskebølvatnet presented in this study are available on-line through the World Data Center for Paleoclimatology (http://www.ncdc.noaa.gov/paleo/pubs/jopl2012arctic/jopl2012arctic.html).

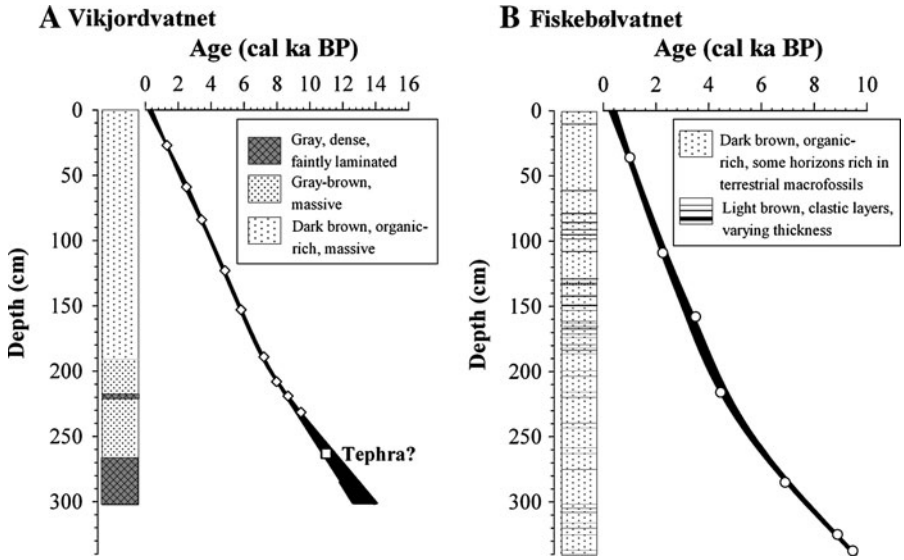

Fig. 3 Sediment stratigraphy and age-depth models for sediment cores from Vikjordvatnet (**a**) and Fiskebølvatnet (**b**). Age-depth models are smooth spline functions fitted to each set of ages (Table 1) using the Clam routine (Blaauw 2010). The 95 % confidence intervals are indicated by the width of the *black envelope*

(Sigvaldason 2002), which have also been found at the base of a peat deposit in Lofoten (Pilcher et al. 2005). We did not include this tephra horizon in the age model because of uncertainties associated with the low concentration of shards and few geochemical analyses, but this age roughly supports our extrapolated chronology (Fig. 3a). Nevertheless, the majority of the record that spans the Holocene is well constrained and there are no significant changes in sedimentation rate, which averages 0.24 mm/year (42 year/cm).

Sedimentological and biological properties were measured on the Holocene section of the core, the upper 268 cm or the last 11.6 ka (Fig. 4). Aside from the lowest part of the record, the core has an overall high organic-matter content (average OM = 25 %) and low magnetic susceptibility. Changes in the characteristics of the sediment define three main paleoenvironmental phases. During the earliest phase (11.6–7.2 ka), there is a progressive decrease in magnetic susceptibility, Ti, and MAR. The most rapid drop in values occurs from 11.6 to 9.4 ka. δ^{13}C values decrease during this interval from −22.8 to −26.1 ‰. Organic-matter flux increases from 0.03 to 0.12 g/cm^2/year (9–29 % OM) and C/N values rise from 8.4 and then fluctuate between 9.6 and 11.2. The increase in the organic-matter flux is not uniform and includes two periods of decreasing values, 10.9–10.2 ka and 9.2–8.0 ka. At 8.6 ka, there is a sharp decrease in organic-matter content, and an increase in magnetic susceptibility, Ti, and MAR that corresponds with a thin clay layer (Fig. 3a). The second phase (7.2–4.8 ka) is marked by less variability in magnetic susceptibility, organic-matter flux, C/N, Ti, and MAR, although δ^{13}C decreases slightly, by about 1 ‰. During the most recent phase of sedimentation (4.8 ka–present), there is a decreasing trend in organic-matter flux and MAR. δ^{13}C values stabilize at −26.5 ‰ and there is a shift to slightly higher average C/N values. After 2.2 ka, the organic-matter flux shows some high-amplitude changes, which are also reflected in fluctuations of magnetic susceptibility and δ^{13}C.

Fiskebølvatnet

The 340-cm-long core from Fiskebølvatnet consists of dark brown, organic-rich sediment that is punctuated by lighter brown, clastic layers (Fig. 3b). These layers vary in thickness from sub-mm to 0.5 cm scale, with some layers consisting of sand-sized grains. The highest concentration of these layers occurs from 200 to 75 cm (4.2–1.7 ka).

Seven radiocarbon ages define the age-depth model for the core (Fig. 3b). The age-depth model indicates that the record spans the last 9.5 ka. The average 2-σ uncertainty ranges for the smooth spline function average ±0.11 ka for the entire record. The average sedimentation rate is 0.37 mm/year (27 year/cm). Sedimentation rates are 0.25 mm/year (40 year/cm) from 9.5 to 4.5 ka, and increase to 0.52 mm/year (19 year/cm) over the last 4.5 ka.

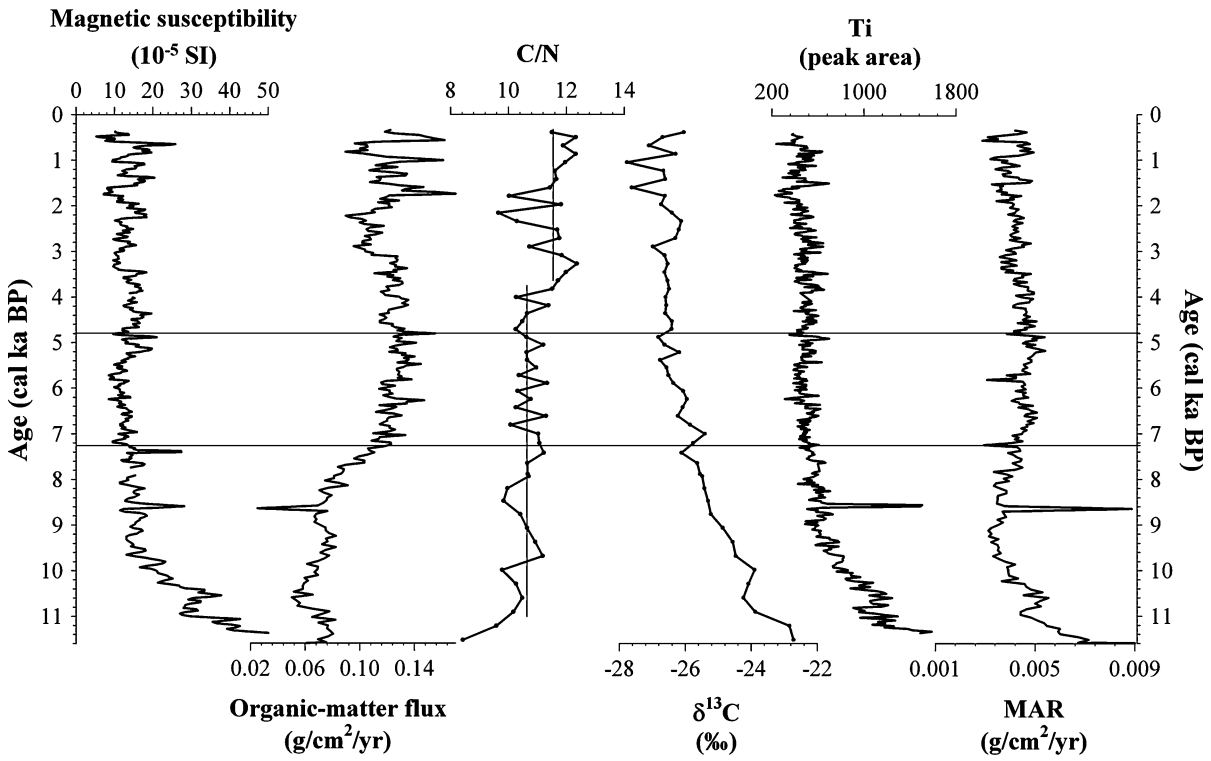

Fig. 4 Properties of the sediment core from Vikjordvatnet, including: magnetic susceptibility, organic-matter flux, C/N, δ^{13}C, Ti, and mass accumulation rate (MAR) over the last 11.6 ka. The *horizontal lines* at 7.3 and 4.8 ka indicate the transitions from the early to mid-Holocene and mid- to late Holocene conditions, respectively

Sedimentological and biological properties of the core from Fiskebølvatnet show high-frequency, high-amplitude variations over the entire 9.5 ka record (Fig. 5). Magnetic susceptibility and Ti display sharp peaks that correspond to decreases in organic-matter content (from 1 to 35 %). Average magnetic susceptibility and Ti values are an order of magnitude higher than in the core from Vikjordvatnet (Fig. 4). Organic-matter flux shows an increasing trend across the record. The most significant long-term changes occur during the last 4.3 ka. At 4.3 ka, there is an increase in sedimentation rates and an abrupt increase in the average MAR followed by many sharp peaks. These changes are also reflected in high magnetic susceptibility and Ti peaks, and an increase in the variability of the organic-matter flux. δ^{13}C and C/N also show shifts in their mean values at 3.5 and 2.9 ka, respectively. Average δ^{13}C values decrease by $\sim$0.6 ‰ after 3.5 ka, and average C/N values increase by $\sim$2 after 2.9 ka (Fig. 5). After 1.7 ka, MAR and magnetic susceptibility show less variability, although average C/N and δ^{13}C values do not change.

Discussion

Interpreting paleoenvironmental conditions

Lake sediment archives are the cumulative product of inorganic and organic input to a lake basin from allochthonous and autochthonous sources. Changes in characteristics of lake sediment through time are a response to regional climate and environmental changes as well as local catchment-scale processes. To better evaluate regional climate conditions in the Lofoten Islands during the Holocene and assess the impact of catchment-scale processes on our lake sediment records, we compare conditions at two lakes with different geomorphic and hydrologic settings. We interpret landscape and lake system changes at Vikjordvatnet and Fiskebølvatnet using magnetic susceptibility, organic-matter flux, C/N, δ^{13}C, Ti concentrations, and MAR.

Magnetic susceptibility and Ti represent changes in minerogenic sediment input from bedrock erosion and clastic sediment transport in the catchment. These

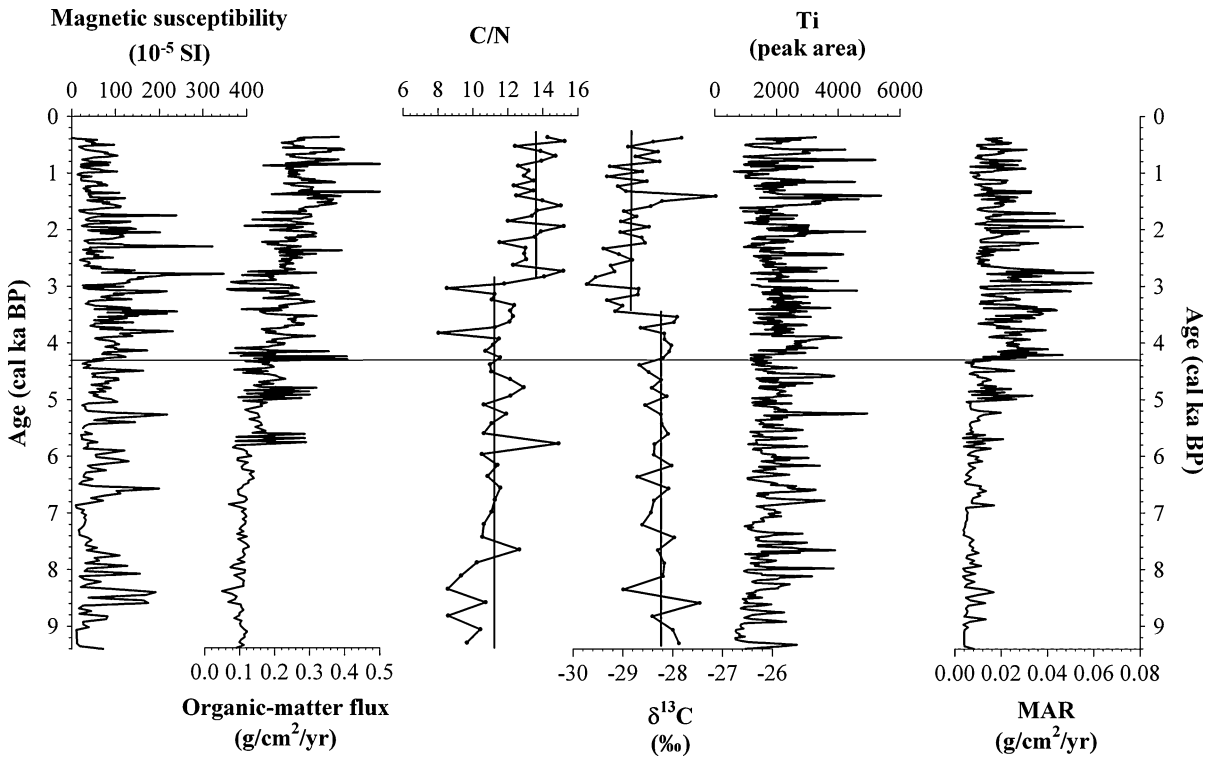

Fig. 5 Properties of the sediment core from Fiskebølvatnet, including: magnetic susceptibility, organic-matter flux, C/N, $\delta^{13}C$, Ti, and mass accumulation rate (MAR) over the last 9.5 ka. The *horizontal line* at 4.3 ka indicates the transition from mid- to late Holocene conditions

parameters have often been measured in marine and lacustrine sediments to rapidly and non-destructively assess relative changes in clastic versus biogenic composition (e.g. Williams et al. 1996; Haug et al. 2001). In Lofoten, the granitic bedrock is a source for both magnetically susceptible and Ti-bearing minerals. Clastic input into a lake basin can be controlled by catchment geomorphology, landscape stability governed by mass-wasting events, soil and vegetation cover, and runoff from rainfall or snowmelt. The organic-matter flux, C/N, and $\delta^{13}C$ are used to characterize organic sedimentation. These parameters can provide information on rates of aquatic productivity, sources of organic matter, and nutrient availability (Meyers 1997, 2003). Organic-matter flux can be a response to changes in primary productivity in the lake driven by nutrient availability, lake water temperature, or changes in the input of terrestrial-derived organic matter. The organic-matter content can also be influenced by dilution with clastic sediment. C/N values provide information on the relative proportion of aquatic versus terrestrial organic matter. C/N values between 4 and 10 are typical of lake algae whereas higher C/N values can be attributed to a greater contribution by terrestrial plants (Meyers 2003). $\delta^{13}C$ values can indicate changes in aquatic productivity, due to the preferential use of the lighter ^{12}C by algae during photosynthesis, but can also indicate changes in the dissolved inorganic carbon available to algae. Lacustrine algae and C_3 land plants typically have $\delta^{13}C$ values in the range of −25 to −30 ‰ (Meyers 1997, 2003).

All of these parameters indicate relative changes in sediment source and supply driven by climate and environmental changes. Since there is not always one paleoenvironmental interpretation for an individual proxy, these parameters need to be evaluated in the context of the local setting and other regional climate reconstructions.

Vikjordvatnet

The sedimentary record from Vikjordvatnet captures the evolution of the lake following deglaciation

(Fig. 4). The clay at the bottom of the core is characteristic of proglacial lake sediment and indicates that a glacier was present in the catchment until ~11.6 ka, although we cannot infer the exact timing of the end of glacial activity due to uncertainty in our age model. Early Holocene (11.6–7.2 ka) changes in sedimentation indicate a response of the lake and catchment to warmer conditions following deglaciation. These are marked by a rapid increase in the organic-matter flux and a decrease in Ti and magnetic susceptibility. Early Holocene warming would have caused increased lake water temperatures, promoting greater aquatic productivity, and vegetation growth and soil formation in the catchment, which stabilized the recently deglaciated landscape and restricted clastic input (Fig. 4). The centennial-scale periods of decreasing organic-matter flux, 10.9–10.2 ka and 9.2–8.0 ka, may have been associated with short-term intervals of cooler and/or wetter conditions that resulted in decreased autochthonous productivity and/or increased clastic input from runoff. However, the catchment became progressively more stable through the early Holocene and these intervals may have been caused by landscape adjustments, such as mass movements due to permafrost melting, which resulted in an increase in clastic input. The decreasing trend in $\delta^{13}C$ values can be explained by processes associated with landscape stabilization. Increasing soil development and establishment of vegetation can lead to progressively greater contributions of isotopically light soil-derived dissolved inorganic carbon (DIC) that is used by algae in the lake during photosynthesis (e.g. Hammarlund 1993). This contrasts with the isotopically heavier DIC that would have been input to the lake immediately following deglaciation, from the weathering of exposed bedrock. Similar trends have been observed in other European lakes following deglaciation (Turney 1999; Nunez et al. 2002).

In Vikjordvatnet during the mid-Holocene (7.2–4.8 ka), the organic-matter flux and other parameters show less variability (Fig. 4). This may be a response to complete landscape stabilization or stable climate conditions following the more significant changes exhibited during the early Holocene.

The late Holocene (4.8 ka–present) is marked by an overall decrease in organic-matter flux and MAR, and a slight increase in C/N (Fig. 4). These changes likely indicate a decrease in autochthonous productivity, which would explain the decline in organic-matter flux, the slight decrease in the proportion of aquatic organic matter relative to terrestrial input exhibited in C/N values, and lower MAR. Decreased productivity during this interval was possibly in response to regional climate cooling. In addition to this trend, there is an increase in the variability of organic-matter flux and magnetic susceptibility after 2.2 ka, which may have resulted from more intense short-term periods of greater runoff.

Fiskebølvatnet

The sedimentary record from Fiskebølvatnet indicates that deposition is dominated by periodic clastic input (Fig. 5). The high elevations, steep slopes, and lower amount of soil and vegetation cover in the catchment allow runoff to carry coarse clastic material to the lake during spring snowmelt, as well as from significant precipitation events. Clastic layers are reflected in high magnetic susceptibility and Ti values, and low organic-matter flux values, resulting from dilution by minerogenic material (Fig. 5). High-frequency and large-amplitude changes in these parameters throughout the record show that these runoff events have been a characteristic feature of this lacustrine system for the last 9.5 ka. The biological parameters do not show as much variability as the physical sediment parameters of Fiskebølvatnet and indicate that the high frequency changes are not associated with large swings in productivity or in the relative input of terrestrial versus aquatic organic matter.

At 4.3 ka abrupt shifts in physical and biological properties indicate an increase in the frequency and intensity of runoff events during the late Holocene. At ~4.3 ka, there was a rapid increase in MAR that was sustained, but highly variable, until ~1.7 ka (Fig. 5). This change was driven by an increase in both sediment density and sedimentation rate, which increased from 0.25 to 0.52 mm/year (Fig. 3). Large peaks in magnetic susceptibility and Ti during this interval result from an increase in the observed grain size of clastic layers, indicating an increase in the energy of runoff events and their ability to carry coarser material to the lake. This period of highly variable sedimentation is clearly seen in the organic-matter flux.

These changes were followed by a shift in organic-matter properties (C/N, $\delta^{13}C$) (Fig. 5). We interpret the direction of change in these parameters as

primarily a result of a relative increase in the proportion of terrestrial-derived organic material. The higher C/N values show there was a greater contribution by terrestrial plants, which are relatively carbon rich and nitrogen poor (Meyers 1997, 2003). This change in the composition of organic matter to more terrestrial sources can also explain the slight decrease in the bulk $\delta^{13}C$ value, as aquatic and terrestrial sources of organic matter can have slightly different $\delta^{13}C$ values if there is a difference in the $\delta^{13}C$ of their inorganic carbon sources. A decrease in lacustrine productivity could also have contributed to lower $\delta^{13}C$ values, as algae discriminate against the heavier carbon isotope (Meyers 1997), and might also explain higher C/N values. However the increase in the organic-matter flux shows that these changes are likely related to the input of more terrestrial organic matter. We attribute this change to increased runoff, which mobilized a greater amount of vegetation in the catchment, increasing terrestrial input to the lake.

After 1.7 ka, the decrease in MAR and magnetic susceptibility peaks likely mark the end of the most intense runoff events (Fig. 5). However, the average MAR remained elevated, there are large Ti peaks and high-amplitude variations throughout this interval, and C/N and $\delta^{13}C$ values remain elevated, indicating that high-energy runoff events persisted, although they may have been of a smaller magnitude than in the preceding interval.

Contrasting response of Fiskebølvatnet and Vikjordvatnet to Holocene climate changes

Vikjordvatnet and Fiskebølvatnet are in two different geomorphological settings and contain sedimentary sequences with contrasting characteristics indicating different responses to Holocene climate changes. Vikjordvatnet is within a low-relief catchment with more complete vegetation cover, and multiple up-valley lakes restricting direct high-energy input (Fig. 2). The sedimentary record spans the Holocene and primarily documents the gradual response of the lake and catchment to early Holocene warming and late Holocene cooling (Fig. 4). By contrast, Fiskebølvatnet is located within a catchment that has high relief and steep slopes, which promotes high-energy transport of material directly from the catchment into the lake (Fig. 2). The sedimentary sequence does not record any gradual early or mid-Holocene environmental changes and is dominated throughout by high-frequency runoff events (Fig. 5). The most significant change in sedimentation occurred during the late Holocene when the frequency and magnitude of runoff events increased. Figure 6 compares organic-matter flux and MAR from each lake record, which exemplify the main environmental changes that impacted each catchment during the Holocene. The transition from the early to mid-Holocene at 7.3 ka is defined by the record from Vikjordvatnet. The transition from the mid- to late Holocene conditions is not synchronous between the two records, although both occurred within the interval from 4.8 to 4.3 ka.

Comparison to regional Holocene climate records

Holocene climate in Fennoscandia is generally characterized by early Holocene warming with a peak during the mid-Holocene, followed by late-Holocene cooling (Snowball et al. 2004; Seppä et al. 2009; Nesje 2009). These trends are well expressed in reconstructed northern Europe atmospheric temperatures (e.g. Seppä et al. 2009), northern North Atlantic sea-surface temperatures (e.g. Calvo et al. 2002), and glacier advances in Norway (Nesje et al. 2008; Nesje 2009). These millennial-scale climate trends are driven by Northern Hemisphere summer insolation, which peaked 12–10 ka and steadily declined during the Holocene (Berger and Loutre 1991).

Early Holocene (11.6–7.3 ka)

The end of glacial activity in the Vikjordvatnet valley is estimated to have occurred at c. 11.6 ka, which generally corresponds with the timing of regional deglaciation. In northern Norway, the end of the Younger Dryas and onset of the early Holocene is marked by the retreat of glaciers in several fjords at c. 10.3 ^{14}C ka BP (11.8 cal ka BP) (Fimreite et al. 2001; Vorren and Plassen 2002; Hald et al. 2003), a rapid increase of SSTs of 3.0–3.5 °C at 11.7 ka (Berner et al. 2010), and a shift to warmer and more stable surface temperature conditions in Andfjord at 11.5 ka (Fig. 1) (Ebbesen and Hald 2004).

Climate of the early Holocene is marked by overall warming as the ice sheet retreated farther inland and temperatures rose in response to insolation changes and the transport of warmer Atlantic Water into the

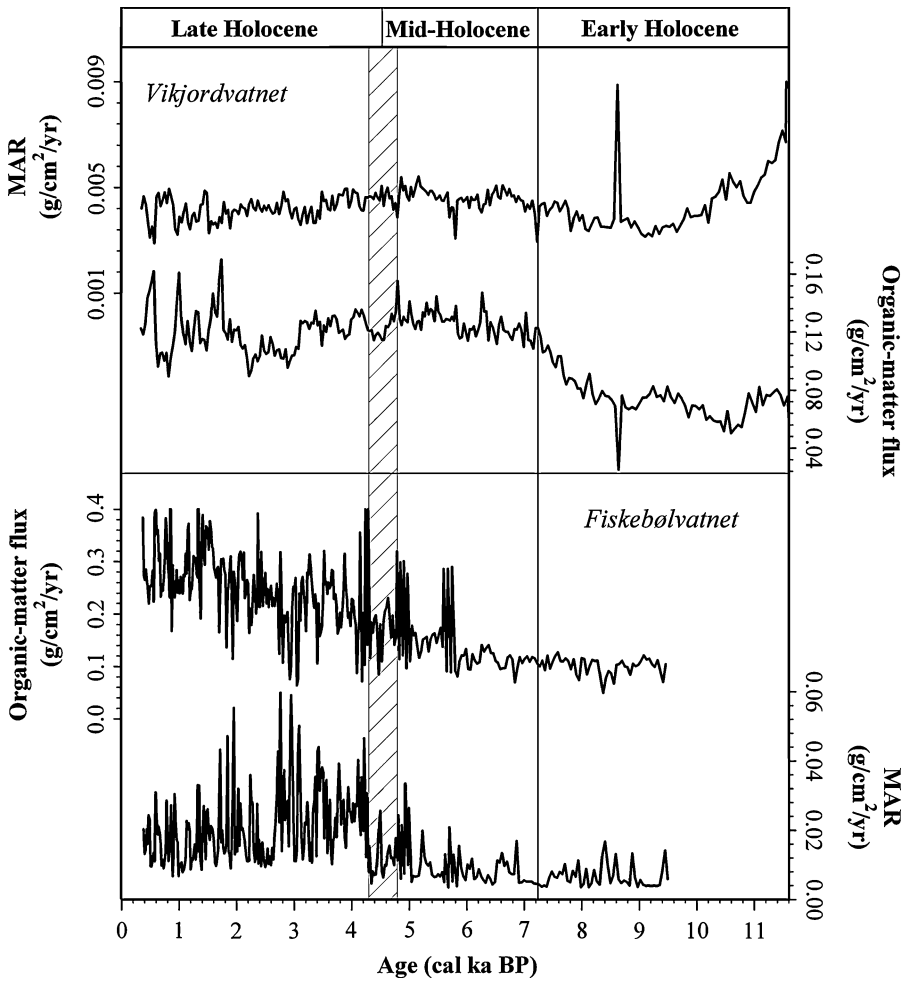

Fig. 6 Comparison of organic-matter flux and mass accumulation rate (MAR) between Vikjordvatnet (*top*) and Fiskebølvatnet (*bottom*). The transition from early and mid-Holocene conditions (7.3 ka), as determined from Vikjordvatnet is indicated by a *vertical line*. The transition from mid- to late Holocene (4.8–4.3 ka) conditions is indicated by the *shaded bar* based on data from Vikjordvatnet and Fiskebølvatnet

Nordic Seas (Hald et al. 2007). During this interval, the record from Vikjordvatnet shows evidence for increased aquatic productivity, soil formation in the catchment, and stabilization of the surrounding landscape from 11.6 to 7.3 ka (Fig. 4).

The overall warming trend in Vikjordvatnet could have been interrupted by centennial-scale cool intervals as indicated by fluctuations in organic-matter flux from 10.9 to 10.2 ka and, more significantly, from 9.2 to 8.0 ka when conditions were cooler and possibly wetter. The period from 10.9 to 10.2 ka in Vikjordvatnet is not well constrained by our age model, but roughly corresponds with a cooling event at 10.3 ka interpreted from records around the North Atlantic region (Björck et al. 2001), the advance of mountain glaciers in southern Norway termed the Erdalen event (Dahl et al. 2002; Nesje et al. 2008; Nesje 2009), and cooling found in eastern Norwegian Sea SST records from 10.3 to 9.9 ka (Berner et al. 2010) possibly related to freshwater forcing and a reduction in thermohaline circulation. The other period, 9.2–8.0 ka in Vikjordvatnet, overlaps with the timing of the "8.2 ka" event. This event is the most dramatic period of cooling observed in Holocene temperature reconstructions from Greenland ice cores (Alley et al. 1997) and it is well-expressed as a period of strong cooling across much of Europe (Alley and Ágústsdóttir 2005). There is also evidence that the 8.2 ka event occurred within a longer interval of climate deterioration from 8.5 to 8.0 ka (Rohling and Pälike 2005). In central and southern Norway, glacier advances are recorded from c. 8.5 to 8.0 cal ka BP, locally called the Finse event (Dahl and Nesje 1994, 1996; Nesje et al. 2008; Nesje 2009), and these were accompanied by a decrease of SSTs in the Norwegian Sea (Risebrobakken et al. 2003; Hald et al. 2007). Records of

glacier activity show this event was associated with a period of greater winter precipitation from 9.2 to 8.3 cal ka BP (Nesje et al. 2001). Terrestrial paleoclimate records from northern Fennoscandia lack strong evidence for cooling linked to the 8.2 ka event (Seppä et al. 2007), although there is evidence for glacier advances in northern Norway prior to this period, from 9.8 to 9.4 ka and 9.3 to 8.9 ka (Bakke et al. 2005), and some temperature reconstructions from northern Sweden also show cooling (Korhola et al. 2000; Rosén et al. 2001).

Mid-Holocene (7.3–4.8 ka)

In Vikjordvatnet, organic-matter concentrations stabilized and it appears that vegetation development and the catchment stabilized between 7.3 and 4.8 ka. Maximum summer temperatures in this region were reached during the mid-Holocene (c. 8.0–5.0 ka) (Snowball et al. 2004; Seppä et al. 2009). Pollen records indicate temperatures were 1.5–2.0 °C higher than present (Bjune et al. 2004, 2005). SSTs reconstructions based on diatoms (Andersen et al. 2004) and alkenones (Calvo et al. 2002) from core MD95-2011 also exhibit a pronounced Holocene thermal maximum, and most glaciers in Norway completely melted away sometime between 8.0 and 4.0 ka (Nesje et al. 2008; Nesje 2009; Bakke et al. 2010). A record of summer surface wetness assessed from carbon and hydrogen isotope ratios of leaf waxes and *Sphagnum* biomarkers in a peat deposit from Lofoten indicates this was a dry period (Nichols et al. 2009).

Late Holocene (4.8 ka–present)

The late Holocene was marked by overall decreasing summer temperatures in response to a decrease in summer insolation (Snowball et al. 2004; Seppä et al. 2009). This period was associated with the rejuvenation and gradual expansion of glaciers (Nesje et al. 2008; Nesje 2009). The alkenone SST record from core MD95-2011 indicates a stepped decrease in temperatures at 5.5 ka and again at 2.7 ka (Calvo et al. 2002). The late Holocene was also characterized by wetter conditions during summer and winter, as indicated by the hydrologic record based on biomarkers from Lofoten (Nichols et al. 2009) and records of glacial activity from northern Norway (Bakke et al. 2005, 2008).

The reconstructions based on sediments from Vikjordvatnet show evidence for colder conditions and Fiskebølvatnet indicates increased runoff during the late Holocene (Fig. 6). In Vikjordvatnet, after 4.8 ka, there is evidence for decreased aquatic productivity that likely reflects a response to lower temperatures. The onset of changes in Fiskebølvatnet is defined by an increase in the influx clastic material at 4.3 ka. Fiskebølvatnet shows the greatest input from runoff beginning at 4.3 ka and lasting until 1.7 ka. This interval closely corresponds with the period of increased winter precipitation, from 3.8 to 2.0 ka, interpreted from reconstructed glacier equilibrium-line altitudes from the Lyngen Peninsula (Bakke et al. 2008) and an increase in winter precipitation from 4.0 to 2.3 ka interpreted from enhance minerogenic influx into another lacustrine system in northern Norway (Janbu et al. 2011).

Conclusions

The sedimentary records from Vikjordvatnet and Fiskebølvatnet provide detailed information on the different responses of two lake systems that experienced the same regional changes in Holocene climate. Paleoenvironmental interpretations were based on magnetic susceptibility, organic-matter flux, C/N, $\delta^{13}C$, Ti concentrations, and MAR. Both records show distinct phases of sedimentation during the Holocene that generally correspond with the timing of major climate transitions recorded by other paleoclimate records from the region. Vikjordvatnet provides evidence for warming and landscape stabilization following deglaciation during the early to mid-Holocene (11.6–7.2 ka) in response to higher summer insolation and increasing inflow of warm Atlantic water into the Norwegian Sea. Instability during the early Holocene warming was also observed as short-term decreases in the organic-matter content of the sediment from 10.9 to 10.2 ka and 9.2 to 8.0 ka. These may correspond to regional cooling events, which have been attributed to freshwater forcing and a slowdown of the northward transport of warm Atlantic water. The interval overlapping the regional Holocene thermal maximum is marked by high organic-matter content and stable conditions from 7.3 to 4.8 ka. This is followed by the transition to a cooler late Holocene. The transition to the late Holocene in data from

Fiskebølvatnet is expressed as an abrupt onset to wetter conditions at 4.3 ka, marked by an increase in the magnitude and frequency of high-energy runoff events. This trend corresponds with glacial records that indicate increased winter precipitation driven by more frequent westerly circulation. The onset of late Holocene conditions is not synchronous between Vikjordvatnet and Fiskebølvatnet, although it occurred within the interval from 4.8 to 4.3 ka. The difference in timing between the two records might be the result of the different physical response of each catchment to environmental change.

Acknowledgments This project was funded by National Science Foundation grants ARC-0714074 and ARC-0909354. Support was also provided by a US Fulbright Program Fellowship to NLB. We thank Jostein Bakke, Sarah Balascio, William D'Andrea, Bjørn Kvisvik, and Lucien von Gunten for help with fieldwork, Diana Barrett for assistance in processing sediment cores, and Finn Unstad, Geir Are Johansen, and Svein-Bjarne Olsen for logistical support in Lofoten. We also thank Pierre Francus, Jonathan Woodruff, Julie Brigham-Grette, Darrell Kaufman, and three anonymous reviewers for comments on earlier drafts.

References

Alley RB, Ágústsdóttir AM (2005) The 8 k event: cause and consequences of a major Holocene abrupt climate change. Quat Sci Rev 24:1123–1149

Alley RB, Mayewski PA, Sowers T, Stuiver M, Taylor KC, Clark PU (1997) Holocene climate instability: a prominent, widespread event 8200 yr ago. Geology 25:483–486

Andersen C, Koç N, Jennings A, Andrews JT (2004) Nonuniform response of the major surface currents in the Nordic Seas to insolation forcing: implications for the Holocene climate variability. Paleoceanography 19:PA2003

Bakke J, Dahl SO, Paasche Ø, Løvlie R, Nesje A (2005) Glacier fluctuations, equilibrium-line altitudes and paleoclimate in Lyngen, northern Norway, during the Lateglacial and Holocene. The Holocene 15:518–540

Bakke J, Lie Ø, Dahl SO, Nesje A, Bjune AE (2008) Strength and spatial patterns of the Holocene wintertime westerlies in the NE Atlantic region. Glob Planet Change 60:28–41

Bakke J, Dahl SO, Paasche Ø, Simonsen JR, Kvisvik B, Bakke K, Nesje A (2010) A complete record of Holocene glacier variability at Austre Okstindbreen, northern Norway: an integrated approach. Quat Sci Rev 29:1246–1262

Balascio NL (2011) Lacustrine records of Holocene climate and environmental change from the Lofoten Islands, Norway. Ph.D. Dissertation. University of Massachusetts, Amherst

Berger A, Loutre MF (1991) Insolation values for the climate of the last 10 million years. Quat Sci Rev 10:297–317

Berner KS, Koç N, Godtliebsen F (2010) High frequency climate variability of the Norwegian Atlantic current during the early Holocene period and possible connection to the Gleissberg cycle. The Holocene 20:245–255

Berner KS, Koç N, Godtliebsen F, Divine D (2011) Holocene climate variability of the Norwegian Atlantic current during high and low solar insolation forcing. Paleoceanography 26:PA2220

Bigler C, Larocque I, Peglar SM, Birks HJB, Hall RI (2002) Quantitative multiproxy assessment of long-term patterns of Holocene environmental change from a small lake near Abisko, northern Sweden. The Holocene 12:481–496

Bigler C, Grahn E, Larocque I, Jeziorski A, Hall RI (2003) Holocene environmental change at Lake Njulla (999 m a.s.l.), northern Sweden: a comparison with four small nearby lakes along an altitudinal gradient. J Paleolimnol 29:13–29

Bigler C, Barnekow L, Heinrichs ML, Hall RI (2006) Holocene environmental history of Lake Vuolep Njakajaure (Abisko National Park, northern Sweden) reconstructed using biological proxy indicators. Veg Hist Archaeobot 15:309–320

Birks CJA, Koç N (2002) A high-resolution diatom record of late-quaternary sea-surface temperatures and oceanographic conditions from the eastern Norwegian Sea. Boreas 31:323–344

Björck S, Muscheler R, Kromer B, Andresen CS, Heinemeier J, Johnsen J, Johnsen SJ, Conley D, Koç N, Spurk M, Veski S (2001) High-resolution analyses of an early Holocene climate event may imply decreased solar forcing as an important climate trigger. Geology 29:1107–1110

Bjune AE, Birks HJB (2008) Holocene vegetation dynamics and inferred climate changes at Svanåvatnet, Mo i Rana, northern Norway. Boreas 37:146–156

Bjune AE, Birks HJB, Seppä H (2004) Holocene vegetation and climate history on a continental-oceanic transect in northern Fennoscandia based on pollen and plant macrofossils. Boreas 33:211–223

Bjune AE, Bakke J, Nesje A, Birks HJB (2005) Holocene mean July temperature and winter precipitation in western Norway inferred from palynological and glaciological lake-sediment proxies. The Holocene 15:177–189

Blaauw M (2010) Methods and code for 'classical' age-modelling of radiocarbon sequences. Quat Geochronol 5: 512–518

Bradley RS (2008) Holocene perspectives on future climate change. In: Battarbee RW, Binney HA (eds) Natural climate variability and global warming—a holocene perspective. Wiley, London, pp 254–268

Calvo E, Grimalt JO, Jansen E (2002) High resolution U-37(K) sea surface temperature reconstruction in the Norwegian Sea during the Holocene. Quat Sci Rev 21: 1385–1394

Corbett LB, Munroe JS (2010) Investigating the influence of hyrdogeomorphic setting on the response of lake sedimentation to climatic changes in the Uinta Mountains, Utah, USA. J Paleolimnol 44:311–325

Dahl SO, Nesje A (1994) Holocene glacier fluctuations at Hardangerjøkulen, central-southern Norway: a high resolution composite chronology from lacustrine and terrestrial deposits. The Holocene 4:269–277

Dahl SO, Nesje A (1996) A new approach to calculating Holocene winter precipitation by combining glacier equilibrium-line altitudes and pine-tree limits: a case study

from Hardangerjøkulen, central southern Norway. The Holocene 6:381–398

Dahl SO, Nesje A, Lie O, Fjordheim K, Matthews JA (2002) Timing, equilibrium-line altitudes and climatic implications of two early Holocene glacier readvances during the Erdalen Event at Jostedalsbreen, western Norway. The Holocene 12:17–25

Dean WE (1974) Determination of carbonate and organic matter in calcareous sediments and sedimentary rocks by loss on ignition: comparison with other methods. J Sediment Petrol 44:242–248

Ebbesen H, Hald M (2004) Unstable Younger Dryas climate in the northeast North Atlantic. Geology 32:673–676

Fimreite S, Vorren K, Vorren TO (2001) Vegetation, climate and ice-front oscillations in the Tromsø area, northern Norway during the Allerød and Younger Dryas. Boreas 30:89–100

Hald M, Husum K, Vorren TO, Grøsfjeld K, Jensen HB, Sharapova A (2003) Holocene climate in the subarctic fjord Malangen, northern Norway: a multi-proxy study. Boreas 32:543–559

Hald M, Andersson C, Ebbesen H, Jansen E, Klitgaard-Kristensen D, Risebrobakken B, Salomonsen GR, Sarnthein M, Sejrup HP, Telford RJ (2007) Variations in temperature and extent of Atlantic Water in the northern North Atlantic during the Holocene. Quat Sci Rev 26:3423–3440

Hammarlund D (1993) A distinct $\delta^{13}C$ decline in organic lake sediments at the Pleistocene-Holocene transition in southern Sweden. Boreas 22:236–243

Haug GH, Hughen KA, Sigman DM, Peterson LC, Röhl U (2001) Southward migration of the intertropical convergence zone through the Holocene. Science 293:1304–1308

Heinrichs M, Barnekow L, Rosenberg S (2006) A comparison of chironomid biostratigraphy from Lake Vuolep Njakajaure with vegetation, lake-level, and climate changes in Abisko National Park, Sweden. J Paleolimnol 36:119–131

Hopkins TS (1991) The GIN sea—a synthesis of its physical oceanography and literature review 1972–1985. Earth Sci Rev 30:175–318

Hurrell JW, Dickson RR (2004) Climate variability over the North Atlantic. In: Stenseth NC, Ottersen G, Hurrell JW, Belgrano A (eds) Marine ecosystems and climate variation: the North Atlantic: a comparative perspective. Oxford University Press, Oxford, pp 15–31

Janbu AD, Paasche Ø, Talbot MR (2011) Paleoclimate changes inferred from stable isotopes and magnetic properties of organic-rich lake sediments in Arctic Norway. J Paleolimnol 46:29–44

Kaufman DS, Ager TA, Anderson NJ, Anderson PM, Andrews JT, Bartlein PJ, Brubaker LB, Coats LL, Cwynar LC, Duvall ML, Dyke AS, Edwards ME, Eisner WR, Gajewski K, Geirsdóttir A, Hu FS, Jennings AE, Kaplan MR, Kerwin MW, Lozhkin AV, MacDonald GM, Miller GH, Mock CJ, Oswald WW, Otto-Bliesner BL, Porinchu DF, Rühland K, Smol JP, Steig EJ, Wolfe BB (2004) Holocene thermal maximum in the western Arctic (0–180°W). Quat Sci Rev 23:529–560

Korhola A, Weckström J, Holmström L, Erästö P (2000) A quantitative Holocene climate record from diatoms in northern Fennoscandia. Quat Res 54:284–294

Korhola A, Vasko K, Toivonen HTT, Olander H (2002) Holocene temperature changes in northern Fennoscandia reconstructed from chironomids using Bayesian modeling. Quat Sci Rev 21:1841–1860

Larocque I, Bigler C (2004) Similarities and discrepancies between chironomid- and diatom-inferred temperature reconstructions through the Holocene at Lake 850, northern Sweden. Quat Int 122:109–121

Last WM, Smol JP (2001) Tracking environmental change using lake sediments, volume 2: physical and geochemical methods. Kluwer, Dordrecht, p 576

Meyers PA (1997) Organic geochemical proxies of paleoceanographic, paleolimnologic, and paleoclimatic processes. Org Geochem 27:213–250

Meyers PA (2003) Applications of organic geochemistry to paleolimnological reconstructions: a summary of examples from the Laurentian Great Lakes. Org Geochem 34:261–289

Miller GH, Brigham-Grette J, Alley RB, Anderson L, Bauch HA, Douglas MSV, Edwards ME, Elias SA, Finney BP, Fitzpatrick JJ, Funder SV, Herbert TD, Hinzman LD, Kaufman DS, MacDonald GM, Polyak L, Robock A, Serreze MC, Smol JP, Spielhagen R, White JWC, Wolfe AP, Wolff EW (2010) Temperature and precipitation history of the Arctic. Quat Sci Rev 29:1679–1715

Møller JJ (1985) Coastal caves and their relation to early postglacial shore levels in Lofoten and Vesterålen, North Norway. Nor Geol Unders 400:51–65

Nesje A (2009) Latest Pleistocene and Holocene alpine glacier fluctuations in Scandinavia. Quat Sci Rev 28:2119–2136

Nesje A, Lie O, Dahl SO (2000) Is the North Atlantic oscillation reflected in Scandinavian glacier mass balance records? J Quat Sci 15:587–601

Nesje A, Matthews JA, Dahl SO, Berrisford MS, Andersson C (2001) Holocene glacier fluctuations of Flatebreen and winter precipitation changes in the Jostedalsbreen region, western Norway, based on glaciolacustrine records. The Holocene 11:267–280

Nesje A, Bakke J, Dahl SO, Lie Ø, Matthews M (2008) Norwegian mountain glaciers in the past, present and future. Glob Planet Change 60:10–27

Nichols JE, Walcott M, Bradley R, Pilcher J, Huang Y (2009) Quantitative assessment of precipitation seasonality and summer surface wetness using ombrotrophic sediments from an Arctic Norwegian peatland. Quat Res 72:443–451

Nunez R, Spiro B, Pentecost A, Kim A, Coletta P (2002) Organo-geochemical and stable isotope indicators of environmental change in a marl lake, Malham Tarn, NorthYorkshire, U.K. J Paleolimnol 28:403–417

Pilcher J, Bradley RS, Francus P, Anderson L (2005) A Holocene tephra record from the Lofoten Islands, Arctic Norway. Boreas 34:136–156

R Development Core Team (2011) R: a language and environment for statistical computing. R Foundation for Statistical Computing, Vienna, Austria. www.R-project.org

Reimer PJ, Baillie MGL, Bard E, Bayliss A, Beck JW, Blackwell PG, Bronk Ramsey C, Buck CE, Burr GS, Edwards RL, Friedrich M, Grootes PM, Guilderson TP, Hajdas I, Heaton TJ, Hogg AG, Hughen KA, Kaiser KF, Kromer B, McCormac FG, Manning SW, Reimer RW, Richards DA, Southon JR, Talamo S, Turney CSM, van der Plicht J,

Weyhenmeyer CE (2009) IntCal09 and Marine09 radiocarbon age calibration curves, 0–50,000 years cal BP. Radiocarbon 51:1111–1150

Risebrobakken B, Jansen E, Andersson C, Mjelde E, Hevroy K (2003) A high-resolution study of Holocene paleoclimatic and paleoceanographic changes in the Nordic Seas. Paleoceanography 18:1017

Rohling EJ, Pälike H (2005) Centennial-scale climate cooling with a sudden cold event around 8,200 years ago. Nature 434:975–979

Rosén P, Segerström U, Eriksson L, Renberg I, Birks HJB (2001) Holocene climatic change reconstructed from diatoms, chironomids, pollen and near-infrared spectroscopy at an alpine lake (Sjuodjijaure) in northern Sweden. The Holocene 11:551–562

Rubensdotter L, Rosqvist G (2003) The effect of geomorpholocial setting on Holocene lake sediment variability, northern Swedish Lapland. J Quat Sci 18:757–767

Rubensdotter L, Rosqvist G (2009) Influence of geomorphological setting, fluvial-, glaciofluvial and mass-movement processes on sedimentation in alpine lakes. The Holocene 19:665–678

Seppä H, Birks HJB (2001) July mean temperature and annual precipitation trends during the Holocene in the Fennoscandian tree-line area: pollen-based climate reconstructions. The Holocene 11:527–539

Seppä H, Birks HJB (2002) Holocene climate reconstructions from the Fennoscandian tree-line area based on pollen data from Toskaljavri. Quat Res 57:191–199

Seppä H, Birks HH, Birks HJB (2002) Rapid climatic changes during the Greenland stadial 1 (Younger Dryas) to early Holocene transition on the Norwegian Barents Sea coast. Boreas 31:215–225

Seppä H, Birks HJB, Giesecke T, Hammarlund D, Alenius T, Antonsson K, Bjune AE, Heikkilä M, MacDonald GM, Ojala AEK, Telford RJ, Veski S (2007) Spatial structure of the 8200 cal yr BP event in northern Europe. Clim Past 3:225–236

Seppä H, Bjune AE, Telford RJ, Birks HJB, Veski S (2009) Last nine-thousand years of temperature variability in Northern Europe. Clim Past 5:523–535

Sigvaldason GE (2002) Volcanic and tectonic processes coinciding with glaciations and crustal rebound: an early Holocene rhyolitic eruption in the Dyngjufjöll volcanic centre and the formation of the Askja caldera, north Iceland. Bull Volcanol 64:192–205

Snowball I, Korhola A, Briffa KR, Koç N (2004) Holocene climate dynamics in Fennoscandia and the North Atlantic. In: Battarbee RW, Gasse F, Stickley CE (eds) Past climate variability through Europe and Africa, volume 6: developments in paleoenvironmental research. Springer, Dordrecht, pp 465–494

Stuiver M, Reimer PJ (1993) Extended 14C database and revised CALIB radiocarbon calibration program. Radiocarbon 35:215–230

Turney CSM (1999) Lacustrine bulk organic δ13C in the British Isles during the Last Glacial-Holocene transition (14–9 ka 14C BP). Arct Antarct Alp Res 31:71–81

Tveten E (1978) Geologisk kart over Norge, berggrunnskart Svolvær 1:250 000. Norges Geologiske Undersøkelse

Uvo CB (2003) Analysis and regionalization of northern European winter precipitation based on its relationship with the North Atlantic Oscillation. Int J Climatol 23: 1185–1194

Vorren TO, Plassen L (2002) Deglaciation and paleoclimate of the Andfjord-Vågsfjord area, north Norway. Boreas 31:97–125

Vorren TO, Vorren K-D, Alm T, Gulliksen S, Løvlie R (1988) The last deglaciation (20,000 to 11,000 B.P.) on Andøya, northern Norway. Boreas 17:41–77

Williams T, Thouveny N, Creer KM (1996) Palaeoclimatic significance of the 300 ka mineral magnetic record from the sediments of Lac du Bouchet, France. Quat Sci Rev 15:223–235